Numerical Modelling of the Flow in a Swelling Preform During LCM Mould Filling

Shivam Salokhe[1] Mohammad Rahmati[1] Ryan Masoodi[2]

[1] Faculty of Engineering and Environment, Northumbria University, Newcastle Upton Tyne, NE1 8ST, United Kingdom

[2] School of Design and Engineering, Thomas Jefferson University, 4201 Henry Ave, Philadelphia PA 19144, USA

Abstract

Composite industry increasingly use natural fibres because of their environment-friendly advantages. These natural fibres may swell during the mould filling process when they absorb resin, and this swelling reduces the porosity and permeability of the preform. Hence, computational modelling of the flow in swelling porous media would be useful to model the different mould filling processes with the swelling effect. This paper demonstrates the possibility of using CFD to study the effect of swelling on LCM mould filling in isotropic and orthotropic porous media. An empirical relation for local permeability changes is used to to model the flow of resin under constant volume flow rate and constant injection pressure conditions. The flow front locations and inlet pressure predicted by the CFD simulations are in good agreement with the experimental data for 1-D rectilinear flow case. Further, to capture the flow patterns, two different arrangements employing point injection are considered. t was observed that the volume fraction of resin in swelling porous medium is 6% less than rigid porous medium at any given time. It was also observed that the location of the inlet and outlet has a considerable effect on the flow front advancement.

Keywords *Porous media, swelling, permeability, the volume of fluid method, liquid composite moulding, Darcy law*

Corresponding author:

Ryan Masoodi, School of Design and Engineering, Thomas Jefferson University, 4201 Henry Ave, Philadelphia PA 19144, USA, Email: ryan.masoodi@jefferson.edu

1 Introduction

Liquid composite moulding (LCM) is a cost-effective method for making the net-shaped polymer composite parts. The LCM process includes RTM (Resin Transfer Moulding), VARTM (Vacuum assisted), and other technologies. LCM processes consist of placing several layers of a preform (which is generated by a dry fibrous medium) into a mould. Subsequently, a low viscosity thermoset resin mixed with hardener is injected into the mould cavity until the fibres are saturated and the mould is full. The matrix is then cured and unmoulded. The quality of the LCM parts is heavily dependent on the efficiency and completeness of the mould filling process.[1]

In the past few decades, industries have started to replace the use of synthetic or glass fibers in polymer composites with natural fibres (e.g., jute, kenaf, flax, henequen) because of their environmentally friendly advantages (biodegradability, enhanced energy recovery, reduced tool wear in machining operations).The use of biocomposites is very attractive for automotive industries because of their lower density and cost as compared to glass-reinforced composites and acceptable mechanical properties .[2] However, studies have shown that the plant fibres such as jute can swell significantly when exposed to some liquids, and this swelling influences the porosity and permeability of the porous media and adds a new dimension to model the resin flow through preforms.[3, 4]

The numerical modelling of LCM processes has been used by many researchers to determine the optimal process parameters such as inlet gates and vents and to minimize the total mould filling time.[5] Researchers adopted different numerical methods to study the different LCM process. The LCM mould filling process is usually considered as the moving boundary problem while numerical modelling. The LCM mould filling process can be modelled by using two basic approaches. The first approach is the moving mesh approach, in which the domain near the liquid flow front is re-meshed during each time step.[6] Coulter et al.[7] developed the numerical code based on the on the boundary-fitted coordinate finite difference method and on the homogenized porous media approach to simulate the two-dimensional isothermal resin flow. A numerical model based on the boundary element method is proposed by the Yo and lee [8] and Um and lee [9] to simulate the mould filling process. Chang and Hourng et.al[10] proposed the numerical model based on the Finite Element Method to study the non-isothermal and isothermal mould filling but the applications were limited to the rectangular mould geometries. All these numerical models mentioned above are based on the moving mesh approach. The

accuracy of moving mesh approach is good, but major barrier in numerical modelling was the huge computational cost because, the numerical model with few thousand elements required many hours of the calculation. Also,it became difficult to handle the cases where multiple injection gates and inserts are used [6].

The second approach is the fixed mesh approach, where the liquid flow front tracking is done on the fixed unique mesh throughout the simulation. It is based on the finite element (FE) and control volume (CV) method. This method become computationally efficient to model the mould filling process as a result of recent developments in computing one does not need to re-mesh the domain since the fixed mesh is used [6]. Trouchu.et.al[11] developed the numerical model based on nonconforming finite elements to simulate the mould filling process. The flow front tracking in this method has been done using fixed mesh scheme. Shojaie et.al[12, 13] used Finite element control volume (FE/CV) method for the mould filling simulations. In their work the pressure eqution was solved using finite element formulation while the flow front tracking was done using control volume formulation.Lately, The FE/CV method became the base for the commercial software packages such as PORE FLOW, LIMS, RTM-Worx and PAM-RTM which has been applied for the non-isothermal flow[14]. Silva et al.[15] adopted a numerical simulation methodology that involves multiphysics and multiphase flow modelling using Finite difference and Finite volume methods.

An alternative to the FE/CV approach is the Eulerian free surface modelling techniques to specify the flow front advancement. The volume of fluid method (VOF) is another method used by researchers to simulate the LCM processes. Porto et al.[16] developed a CFD model based on VOF method to simulate the RTM (Resin Transfer Moulding) and LRTM (Light Resin Transfer Moulding). The study is focused on the mould filling times in both processes. The results showed that due to higher-pressure gradient, the LRTM process has less mould filling time than RTM. Yang et al.[17] developed a 3D model for the compression resin transfer moulding (CRTM) using VOF and dynamic mesh model. The resin flow is modelled by means of adding source terms to the standard code. Using a similar approach, Yang et al.[18] proposed a 3-D model for the resin infusion process. In both studies, the thickness of the preform is taken as variable in the process, which leads to the use of dynamic mesh method to account for the changes in preform porosity and permeability.

The adoption of swelling effect into numerical simulation is rarely studied. Masoodi et al.[19] used FE/CV based numerical simulations to study the effect of fibre swelling on the fluid flow

in porous media. In their first efforts, a computer programme (based on the FE/CV approach) is used to model the wicking process in swelling porous media. The simulation utilised a novel form of the continuity equation, which included the effect of liquid absorption and fibre swelling in conjunction with Darcy's law to track the flow front. They proposed a new method for estimation of the time-varying permeability which was used to modify the permeability of the element behind moving flow front. The thickness of the porous media (paper) was not constant as a result of swelling; however, the thickness of porous media is constant in LCM. Also, the permeability is assumed to be a function of time only. This limits the application of these approaches while simulating the LCM mould-fill process.

Masoodi et al.[20] in further efforts, assumed constant thickness of porous media and non-homogenous form of permeability to simulate the LCM mould fill process. The non-homogeneous local permeability and porosity functions are proposed which are based on the wetting time of fabric (porous media) that is $K=K(x, t)$. The two common LCM cases (constant flow rate and constant injection pressure) are studied. The limitation of their studies is that only 1-D cases are considered. A similar study is conducted by Francucci et al.[21] using finite element and volume of fluid method, but it was also limited to 1-D constant injection pressure case. Although the numerical study of LCM mould filling process has been performed for a long time, there is still a lack of numerical models to simulate the flow in 2-D swelling porous media. Some studies considered the porosity as a function of process parameters, such as compression forces. Hence, the adaption of fibre swelling effect into numerical simulation is crucial for the successful design of the mould and will help to eliminate trial and error, which are time consuming and costly. Another group of researchers developed a two-phase flow model to track the wicking flow in swelling porous media. The predicted results showed good agreement with experimental data, but the mathematical model requires several fitting parameters. A specific set of experiments is needed to calculate these parameters, limiting its applications.[22]

As is clear from the reviewed literature, the 2-D and 3-D simulation of flow through swelling porous media are not published yet. The majority of the work is focused on the modelling of the LCM processes, considering the preform to be rigid. Few studies have demonstrated the use of deformable preform into the simulation to model the actual moulding process. Finally, the modelling of the flow in swelling porous medium is rarely studied.

In this article, a numerical methodology is presented to simulate the flow in 2-D swelling porous media. Two injection conditions (constant injection pressure and constant volume flow

rate) are considered to study the effect of fibre swelling on flow front locations and inlet pressure changes. ANSYS Fluent is used to simulate the resin flow in a rectangular mould, which is validated against available experimental data and some published CFD results. Further, the suggested numerical simulations are used to model the flow in 2-D isotropic and orthotropic porous media. The present work is based on a simple approach that alters the permeability in each porous cell zone (cell threads) as time progresses forward. . In this approach, the solver checks if the cell zones are fully saturated or not, then it accordingly modifies the permeability values in each cell zone. Since the present method is based on the finite volume method, it can be used for mould filling simulations for complex components as it allows to use the 3-D, unstructured grids, or even dynamic meshes.

2 Mathematical modelling

In the liquid composite moulding process, the mould is packed with the fibre preforms. It is assumed that throughout the mould filling process, the fibres are in a swelling condition when they absorb the resin and are not shifted by the resin flow. The flow of the resin through the mould is usually slow which can be taken as the inertialess viscous low (Stokes flow). The inertia effect is negligible as the Reynolds of resin flow is less than one, and the effect of surface tension is negligible as compared to the dominant viscous flow. The resin is incompressible, and the filling process is assumed to be isothermal. Hence, based on these assumptions, the problem can be formulated as follows.[6]

2.1 Resin flow during the filling stage

The flow-through fibrous medium has been modelled as the viscous flow through porous media, which is commonly described by the well-known Darcy's law: [23]

$$\vec{u} = -\frac{K}{\mu} \nabla p \qquad (1)$$

where K is the preform permeability, μ is the resin viscosity, p is the fluid pressure, and $\vec{u}$ is the superficial volume averaged flow velocity (Darcy velocity). The relation between superficial velocity and physical velocity is given by,[23]

$$\vec{u} = u\,\varepsilon \qquad (2)$$

where u is the physical velocity of the resin flow and ε is the porosity of porous media. The

single-phase resin flow through rigid porous media can be formulated by employing continuity equation,

$$\nabla.(\vec{u}) = 0 \tag{3}$$

The continuity equation for the resin flow in a liquid absorbing swelling porous matrix is given by,[24]

$$\nabla.(\vec{u}) = -S - \frac{\partial \varepsilon}{\partial t} \tag{4}$$

where the sink term, *S*, is related to the absorption rate of the liquid/resin by fibre matrix. The second term $\left(\frac{\partial \varepsilon}{\partial t}\right)$ is related to the porosity reduction of the fibre matrix as a result of swelling action. If v_f is the total volume fraction of the fibres, the sink term *S* and the rate of increase in fibre volume $\left(\frac{\partial v_f}{\partial t}\right)$ as a result of swelling action can be related using,

$$S = b\frac{\partial v_f}{\partial t} \tag{5}$$

where v_f is fiber volume fraction and b is the absorption coefficient of the fibre matrix that ranges between 0 to 1 (if the increase in total fibre volume is caused by another effect, then the b can be taken beyond unity). Here, $b=1$ case indicates that the rate of increase of fibre matrix volume is equal to the volumetric rate of liquid absorption by fibre matrix and $b=0$ case indicates no absorption of liquid in fibre matrix. Upon using equation (5) in equation (4) and considering the relation $v_f + \varepsilon = 1$, the final continuity equation for the liquid absorbing swelling porous medium is given by,[24]

$$\nabla.(\vec{u}) = (b-1)\frac{\partial \varepsilon}{\partial t} \tag{6}$$

The previous works on the modelling of swelling porous media assumed the value of $b=1$ which lead to acceptable results comparing with the experimental data [19, 20, 25] So for present work, the value of *b* is assumed as 1 for the natural fibres. Hence the equation (6) reduces to equation (3) which will be used to model the flow in the liquid absorbing swelling porous medium. If the absorption coefficient is less than 1 then the revised forms of continuity equation given by equation (6) should be used to model the flow in swelling porous medium.

The momentum equation can be expressed as

$$\frac{\partial}{\partial t}(\rho\vec{u}) + \nabla.(\rho\vec{u}\vec{u}) = -\nabla p + \nabla.(\bar{\bar{\tau}}) + S_i \quad (7)$$

where p *is* the fluid pressure, ρ is the fluid density, $\bar{\bar{\tau}}$ is viscous stress tensor the and S_i is the source term associated with the porous media inputs.[23]

In the source term, conditions are composed of two parts: a viscous loss term and an inertial loss term.[23]

$$S_i = -\left(\frac{\mu}{K}\vec{u} + C_2\frac{1}{2}\rho|\vec{u}|\vec{u}\right) \quad (8)$$

The second term on the left-hand side of equation (7) is the non-linear convection term which can be ignored as Reynold's number related to resin flow in preform is less than 1.[18] On the other hand, the second term in equation (8) can be ignored as the flow is dominated by the viscosity. So, the resulting equation that characterises the resin flow in fibrous preform is given by,[23]

$$\frac{\partial}{\partial t}(\rho\vec{u}) = -\nabla p + \nabla.(\bar{\bar{\tau}}) - \left(\frac{\mu}{K}\vec{u}\right) \quad (9)$$

Equation (9) can be regarded as an extension of the Naiver-stokes equation as a practical way to solve the problems related to the flow in the porous medium. Note that equation (1) or Darcy law is a simplified version of equation (9) or momentum equation.

2.2 Flow cases in LCM mould filling simulations

2.2.1 The constant volume flow rate

For 1-D flow cases, test liquids (resin) are made to flow through the flat rectangular moulds in which the liquid is injected from one side of a rectangular stack of fabric layer (preform. For such flow under constant volume flow rate, the flow front location is given by,[20]

$$X_f = \frac{Q}{\varepsilon A}t \quad (10)$$

where Q is volume flow rate and X_f is the flow front location along the flow direction, t is the filling time, and A is cross-sectional area of the preform. This equation holds valid for both non-swelling porous media and swelling porous media. The consideration of swelling effect is not necessary for the prediction of flow front locations in case of volume flow rate conditions.

According to equation (4), Darcy's velocity behind the moving flow front can be taken as,[20]

$$\frac{d\vec{u}}{dx} = 0 \rightarrow \vec{u} = constant = \frac{Q}{A} \tag{11}$$

To find the pressure field, the constant Darcy's velocity *(u=Q/A)* is substituted into equation (1) which results in,

$$dp = -\frac{Q\mu}{KA}dx \tag{12}$$

Upon integrating the equation (12), the following equation is obtained to predict the inlet pressure for rigid porous media.[20]

$$p_{in} = \frac{\mu}{\varepsilon_o K}\left(\frac{Q}{A}\right)^2 t \tag{13}$$

For swelling porous media, The inlet pressure is function of time but the permeability is a function of the wetting time, which is $K=K(t - t_w)$ for $t > t_w$ where t_w is the time when the local fabric is wetted by the invading liquid and *t* is the time related to current flow front location. Hence the above equation modifies to,

$$p_{in} = \frac{Q^2\mu}{\varepsilon_o A^2}\int_0^t \frac{dt'}{K(t')} \tag{14}$$

Note that in the derivation of equation 14 ,the permeability of perform in wetted region is assumed as homogenious and the function of time only which is $K=K(t)$. However, in practice, it is the function of both space and time. The space dependence of permeability can be expressed in terms of local wetting time values that vary along with flow front

2.2.2 Constant injection pressure condition

In the case of rigid porous media, combining equations (1) and (4) results in the following form of Laplace equation,

$$\nabla^2(p) = 0 \tag{15}$$

Upon solving equation (15) for a 1-D case, and replacing the pressure gradient in equation (1), the flow front location (X_f) for 1-D rigid porous media in case of constant permeability

conditions can be expressed as,[20]

$$X_f = \sqrt{\frac{2P_{in}Kt}{\varepsilon_o \mu}} \tag{16}$$

where P_{in} is the injection pressure and t is the injection time. For swelling porous media, the permeability K is not constant which leads to following elliptic equation for pressure.

$$\nabla(K(\nabla p)) = 0 \tag{17}$$

The expression for flow front locations in case of 1-D swelling porous medium is given by,[20]

$$x_f = \sqrt{\frac{2P_{in}}{\varepsilon_o \mu} \int_0^t K(t')dt'} \tag{18}$$

2.2.3 Permeability function (Experimentally generated)

Natural fibres may swell when they are exposed to liquids such as bio-resins. This phenomenon affects the permeability and the porosity of the porous media. There are some theoretical models available that can be used to estimate the swelling behaviour of fibrous porous media.[24] However, the accuracy of the theoretical models is limited.[20] Therefore, to include the swelling effect in the CFD simulations, a permeability relation that was found experimentally by Masoodi et al.[20] is referred in this study. Following relation was used to measure the permeability

$$K_0 = \frac{Q\mu L}{A\, P_{in}} \tag{19}$$

where K_o is permeability of the preform, μ is the resin viscosity, L is the length of the preform, and P_{in} is the corresponding injection pressure.

The experiments conducted by Masoodi.et.al[20] included permeability measurements for both rigid and swelling conditions. Firstly, the permeability is measured for the rigid conditions and it is taken as the initial permeability (K_0) before the onset of swelling. For the experiments, the motor oil is used as a test liquid and the pressure drop across the preform is measured for the given flow rate value (Q) Since, the oil is typically not absorbed by the jute fibers, it does not induce any changes to porosity and permeability. The permeability is then calculated using the

equation **Error! Reference source not found.**. Note that in the following experiment, since the atmospheric conditions were maintained at outlet, only inlet pressure value is used in equation **Error! Reference source not found.**. The obtained value of permeability for the preform in rigid state was 6×10^{-10} To estimate the changes in permeability due to swelling action, another experiment was conducted. In the same mould, a narrow strip of fabrics, with length of 2.54cm, was inserted where diluted corn syrup (swelling inducing test liquid) was used to flow through it. The pressure at inlet was found to increase due the reduction of the permeability of strip as a result of swelling action. All the measurements are done by assuming the quasi steady state conditions exist inside the strip. The local permeability is then calculated using the equation **Error! Reference source not found.** by measuring the inlet pressure value for any given flow rate at corresponding time values.

Further, the local permeability is then plotted as a function of time as shown in Figure (1), it can be observed that permeability is decreasing as time progresses as a result of fibre swelling in the preform. Equation (20) is a fitting expression that accounts for the changes in local permeability of jute preform (porous medium) when exposed to diluted corn syrup with respect to wetting time *(t)*.[20] The implementation of this relation in CFD simulations is explained in the next section.

$$f(t) = 3.7 \times 10^{-15}t^2 - 1.75 \times 10^{-12} + 6 \times 10^{-10} \quad (20)$$

3 Numerical simulation method

3.1 VOF model for simulating the flow in swelling porous media

The Volume Of Fluid method (VOF) is a surface-tracking technique applied to fixed Eulerian mesh. It is designed for two or more immiscible fluids where the position of the interface between two fluids is of interest. In the VOF method, a single set of momentum equation is shared by the fluids, and the volume fraction for each fluid is tracked in each cell throughout the domain. In this method, the primary and secondary phases (resin and air respectively) are identified by their volume fraction α_a and α_r in a computational cell. If $\alpha_r = 1$, the cell is full of resin; if $\alpha_r = 0$, the cell is full of the other phase (air); and if $0 < \alpha_r < 1$, the cell contains the interface between air and resin.[26]

The velocity for the mixture phase in the volume of fluid method is obtained by the solution of a single set of momentum equation:

$$\frac{\partial}{dt}\left(\rho_{fluid}\vec{u}\right) + \nabla.\left(\rho_{fluid}\vec{u}\vec{u}\right) = -\nabla p + \nabla.\left(\bar{\bar{\tau}}\right) + S_i \qquad (21)$$

Where the subscript fluid refers to the corresponding fluid, which can be any one of two phases or mixture. Assuming the incompressibility, the conservation of mass is described by equation (3). In the volume of the fluid method, the interface between air and resin is tracked by solving the continuity equation for the volume fraction as:

$$\frac{\partial \alpha}{\partial t} + \nabla.\left(\vec{u}\alpha\right) = 0 \qquad (22)$$

where α indicates the volume fraction of the corresponding phase.The effective physical properties of the fluid ϕ (*viscosity* μ_e*, density* ρ_e) in a computational cell are expressed as volume-weighted average:[27]

$$\phi_e(s,t) = \alpha(s,t).\phi_r + [1 - \alpha(s,t)].\phi_a \qquad (23)$$

where *s* indicates the position *(x and y)* and subscript *r* and *a* indicate resin and air respectively. From equations (9), (21) and (23), the VOF model can be established for solving the resin-air two-phase flow in swelling porous media:

$$\frac{\partial}{\partial t}\left(\rho_e\vec{u}\right) = -\nabla p + \nabla.\left(\bar{\bar{\tau}}\right) - \left(\frac{\mu_e}{K}\overrightarrow{u}\right) \qquad (24)$$

3.2 Time and space dependant permeability

Figure 2 shows the schematic arrangement for rectilinear flow, considering the element (porous cell zone) located at x_i from the inlet which gets wet when resin flow front *x* passes through it. The permeability in the wetted region starts to decrease as a result of fibre swelling. If t_w is the time when the element becomes wet, then the following expression holds true for permeability at location x_i

$$(K) = \begin{Bmatrix} K_o & t < t_w \\ f(t - t_w) & t \geq t_w \end{Bmatrix} \qquad (25)$$

Where K_0 is the permeability of dried preform in m^2, *f* is the experimentally estimated function of time for a change in permeability, and *t* is the time in seconds. On combining equations (20) and (25), the final expression that assumes permeability as a function time and space is determined as follows

$$(K) = \begin{Bmatrix} 6 \times 10^{-10} & \boldsymbol{t < t_w} \\ 3.7 \times 10^{-15}(t - t_w)^2 - 1.75 \times 10^{-12}\ (t - t_w) & \\ +6 \times 10^{-10} & \boldsymbol{t \geq t_w} \end{Bmatrix} \quad (26)$$

3.3 Numerical Algorithm

Figure 3 shows the numerical algorithm of the proposed method in which equations (24) and (3) are solved to obtain velocity field.[23] The source term *(Si)* in the equation (24) is modified at each time step via user-defined function based on the equation (26). The computational domain for both cases in this study is a rectangular mould box. The air considered as primary phase and resin is considered as a secondary phase. "The quad type mesh is employed for each simulation". The dimensions and boundary conditions of the computational domain are shown in Figure 4. The details of the of fluid properties, input parameters, solution method, and boundary conditions are summarised in Table 1

3.4 Validation of CFD approach

To perform the mesh sensitivity tests, the CFD results for constant injection pressure, two different computational domains with the dimension of 250×300 (mm) with minimum cell sizes of 0.7 mm and 0.35 mm, are compared. The simulation has been performed for the rectilinear flow with a constant injection pressure of 14 kPa. The flow front locations obtained for both computational domains are shown in Figure 5. It is seen from Figure 5 that the resulting flow front locations for both domains have minor differences. Hence, all computations are done for the domain with cell size as 0.7 mm.

To validate the numerical method, the experimental data for constant volume flow and constant inlet pressure condition are compared with CFD simulations results. The computational domain and important boundary conditions are illustrated in Figure 3. The computational domain is a rectangular box with dimensions of 250×300 (mm), the resin is injected from inlet and air is removed from outlet. To characterise the flow, permeability in both directions *(K_{xx}, K_{yy})* is assumed to be equal.

Figure 6 shows a comparison between experimental data and CFD results for the liquid flow front locations in case of the constant injection pressure condition. Here, the three different injection pressure values *(8 kPa, 12 kPa and 14 kPa)* are used and the permeability is taken as

a function of time and space. It can be seen that the CFD results are in good agreement with the experimental and numerical results by Masoodi et.al.[20] with an average percentage error of 2.7%. Further, Figure 7 shows the experimental and CFD predictions of flow front locations for constant volume flow rate conditions. As previously mentioned in section 2, the effect of swelling does not have a considerable effect while the prediction of flow front locations in case of constant volume flow rate conditions. As expected, the CFD predictions are in good agreement with experimental data.[20] For this case as well, the permeability is assumed to be a function of time and space. Figure 8 shows the evolution of inlet pressure as a function of time for three different flow rates *(Q = 1 ml/s, 2 ml/s and 3 ml/s)*. It is clear from the graphs that predicted results are in good agreement with experimental data [20] with an error margin of 5%. This demonstrates the validity of the present method to model the flow in swelling porous media

4 Results and Discussion

4.1 Two-dimensional mould filling in an isotropic porous media

To explore the ability of the present method to capture the 2-D flow patterns, point type injection instead of boundary type injection is used for simulations. For this purpose, two different cases are considered for the condition of constant injection pressure. Arrangement 1: Central injection arrangement and Arrangement 2: Eccentric injection arrangement. Figure 9 shows the details of the geometry used for both arrangements. The contours of resin volume fraction for 14 kPa injection pressure are shown for both the arrangements for the rigid and swelling condition. Both the cases are simulated for constant injection pressure by assuming the porous domain as isotropic *($K_{xx}=K_{yy}$)* and orthotropic *($K_{xx}=10K_{yy}$)*.

Figures 10 and 11 show the transient contours of resin flow for both arrangements for an isotropic condition. The red colour shows the resin-impregnated region, and the blue colour shows the completely unsaturated region. From the circular injection port, the radial resin flow pattern is observed until it touches the top and bottom walls. The swelling effect is not so dominant in early simulation time (untill 10 sec). As time progresses forward, the swelling effect becomes dominant for both cases, and after t = 30 seconds one can spot the differences in the flow front locations in terms of resin volume fraction. Also, it is observed that, as flow front reaches near to outlet, its advancement becomes slow. It is expected that for larger

dimensions of a porous domain, the swelling effect may be seen as dominant; the reason can be explained from the experimentally generated function for permeability reduction. For higher values of time, the permeability reduces by a higher amount. Also, the position of the inlet gate affects the total mould filling time. It is clear from the Figure 12 that, for central injection point and eccentric injection point the total mould fill time for rigid conditions are 60 seconds and 100 seconds, respectively, and for swelling conditions, these values increase to 70 seconds and 120 seconds respectively. It can be seen from Figure 12 that the advancement of resin flow front is considerably affected by the position of the inlet. There is a considerable difference between trends followed by resin volume fractions for both arrangements. For the case of central injection, the trend is somewhat similar to that of that rectilinear case (see Figure 6 (c)), because in late simulation time the flow front starts to follow the rectilinear case trend, as mentioned in the previous section. Hence one can deduce from these results that the flow front advancement is not greatly affected by the swelling effect in early simulation. The differences in resin volume fractions can be used to design and optimise the LCM processes in terms of numbers, positions, and even size of the inlets.

Also, the ratios of resin volume fraction in swelling condition and the rigid condition is plotted against the time to describe the effect of swelling on flow front propagation. Figure 13 reveals that the ratio of volume fraction shows uneven behaviour after 55 seconds and 40 seconds for central injection and eccentric injection case respectively. As indicated by Figure 10 and 11, for the case of central injection, the flow front reaches to the outlet at around 55-60 seconds. Meanwhile, for the casse of eccentric injection, this time value is around 40 seconds. This uneven behaviour of flow front advancement can be related to the position and size of the outlet. This can be justified by observing Figure 13 (a) and (b): For the case of central injectioncase, the flow front takes more time to reach outlet than the eccentric injection case. The same thing is reflected in the behaviour of the resin volume fraction ratio. One can see that the volume fraction ratio shows a linear behaviour for a longer time for central injection case than eccentric injection. This even behaviour cannot be seen in Figure 12, hence, the results related to resin volume fraction ratio could be helpful while selecting the outlet design and conditions while designing the LCM process.

4.2 Two-dimensional mould filling in an orthotropic porous media

An orthotropic porous medium was considered to evaluate the current approach to simulate the

flow through orthotropic swelling porous media. The permeability in *x*-direction was set ten times higher than in the *y*-direction (i.e., the resin will flow faster in the *x*-direction than *y*-direction). In addition, the overall resistance for this case will be higher than that for the isotropic case, which will result in longer time values for resin flow front to reach mould walls.

Figures 14 and 15 show the resin flow front locations for different times for both geometries to study the effect of distinct permeabilities on flow contours. For this case, the results are shown for 14 kPa injection pressure. Unlike the isotropic case, the resulting pattern for flow front is elliptic. Also, from Figure 16, it is observed that the flow front advancement becomes slow or negligible after 80 seconds. It is expected that, for larger domain sizes and longer simulation time, as mentioned previously, the swelling will become more dominant in both directions; as it increases thesistance in *y*-direction than *x*, so the resulting flow may become closer to 1-D. Hence, it is clear that for orthotropic porous media the size, locations and number of injection ports play a vital role while designing the mould. Further, Figure 17 shows that the resin volume fraction in swelling porous media is about 6% less than rigid porous media, which is related to decreasing permeability due to swelling.

5 Summary and Conclusion

The flow-through swelling porous media during the LCM mould filling process is modelled using the volume of fluid method. A good agreement between CFD and experimental results is obtained for 1-D rectilinear flow case. Also, the CFD predictions for inlet pressure changes for constant volume flow rate conditions showed good agreement with the experimental data. The 2-D transient results demonstrated the applicability of the present model to capture the sharp interface between air and resin under isotropic and orthotropic swelling porous media conditions. The results of this research showed that a computational model based on the finite volume and volume of fluid method can be used to model the flow through swelling porous media by measuring the change in the local permeability as a function of time.

The transient numerical results demonstrated the effect of swelling on the resin flow front advancement in isotropic and orthotropic porous media. The results showed that the advancement of flow front is considerably affected by the position of the inlet and also by the size and location of the outlets. For the orthotropic case, it was observed that the flow front advancement becomes slower due to swelling effect. It was also observed that resin volume fraction in the rigid porous medium is about 6% higher than swelling porous medium. The finite volume method was found to be an efficient and flexible simulation method to model the

flow in swelling porous media during LCM mould filling process. It is expected that these kinds of CFD simulations would help to design and optimise the LCM processes through flow front tracking, choosing the number of inlets and outlets, and prediction of mould filling time. There are also other industrial applications of this method such as modelling the flow in wipes and diapers which are swelling porous substances.

All commercial CFD packages are capable of modelling the flow in rigid and non swelling porous media only .The advantage of the proposed model is that any commercial solver based on the finite volume method can be easily adopted for flow simulation in swelling porous media. The majority of previous studies are based on the assumption of single-phase only while this method uses a multi-phase approach (volume of fluid method) to track the sharp interface between resin and air. It can help to track the smaller interface between air and resin (such as the formation of voids, bubbles, and defects in the process) for different geometries. In the current study, the flow is assumed to be in isothermal condition, but this method can be extended to non-isothermal flow by using either local thermal equilibrium or non-equilibrium models. This method can esily be extended to 3D and can even be used with unstructured or dynamic meshes.

Acknowledgement

The authors would like to thank Jennifer Wilson for editing the manuscript.

References.

1. Wool RP, Khot SN. Bio-Based Resins and Natural Fibers. In: Miracle DB, Donaldson SL, editors. Composites. 21: ASM International; 2001. p. 0.
2. Masoodi R PKM. Modeling the Processing of Natural Fiber Composites Made Using Liquid Composite Molding. Handbook of Bioplastics and Biocomposites Engineering Applications2011. p. 43-73.
3. Rodriguez E, Giacomelli F, Vazquez A. Permeability-porosity relationship in RTM for different fiberglass and natural reinforcements. Journal of composite materials. 2004;38(3):259-68.
4. Umer R, Bickerton S, Fernyhough A. Modelling the application of wood fibre reinforcements within liquid composite moulding processes. Composites Part A: Applied Science and Manufacturing. 2008;39(4):624-39.
5. Zade A, Kuppusamy RRP. Mould fill time sensitivity analysis using isothermal mould filling simulations for applications in liquid composite moulding processes. Materials Today: Proceedings. 2019.
6. Saad A, Echchelh A, Hattabi M, El Ganaoui M. An Optimized Control Volume/Finite Element Method (CV/FEM) for Non-Isothermal Liquid Composite Molding (LCM) Process. In: Driss Z, Necib B, Zhang H-C, editors. Thermo-Mechanics Applications and Engineering Technology. Cham: Springer International Publishing; 2018. p. 81-118.
7. Coulter JP, Guceri SI. Resin Impregnation During the Manufacturing of Composite Materials Subject to Prescribed Injection Rate. Journal of Reinforced Plastics and Composites. 1988;7(3):200-19.
8. Yoo YE, Lee WI. Numerical simulation of the resin transfer mold filling process using the boundary element method. Polymer Composites. 1996;17(3):368-74.
9. Um MK, Lee WI. A study on the mold filling process in resin transfer molding. Polymer Engineering & Science. 1991;31(11):765-71.
10. Chang C-Y, Hourng L-W. Numerical simulation for the transverse impregnation in resin transfer molding. Journal of reinforced plastics and composites. 1998;17(2):165-82.
11. Trochu F, Gauvin R, Gao DM. Numerical analysis of the resin transfer molding process by the finite element method. Advances in Polymer Technology: Journal of the Polymer Processing Institute. 1993;12(4):329-42.
12. Shojaei A, Ghaffarian SR, Karimian SM-H. Numerical simulation of three-dimensional mold filling in resin transfer molding. Journal of reinforced plastics and composites. 2003;22(16):1497-529.
13. Shojaei A, Ghaffarian SR, Karimian SM-H. Numerical analysis of controlled injection strategies in resin transfer molding. Journal

of composite materials. 2003;37(11):1011-35.
14. Bruschke MV, Advani SG. A numerical approach to model non-isothermal viscous flow through fibrous media with free surfaces. International Journal for Numerical Methods in Fluids. 1994;19(7):575-603.
15. Boyard N. Heat Transfer in Polymer Composite Materials: Forming Processes: John Wiley & Sons; 2016.
16. Porto JdS, Letzow M, Santos EDd, Amico SC, Souza JA, Isoldi LA. Computational modeling of RTM and LRTM processes applied to complex geometries. 2012.
17. Yang B, Jin T, Li J, Bi F. Three-Dimensional Numerical Simulation of Mold Filling Process in Compression Resin Transfer Molding. Applied Composite Materials. 2015;22(2):209-30.
18. Yang B, Tang Q, Wang S, Jin T, Bi F. Three-dimensional numerical simulation of the filling stage in resin infusion process. Journal of Composite Materials. 2016;50.
19. Masoodi R, Tan H, Pillai KM. Numerical simulation of liquid absorption in paper-like swelling porous media. AIChE Journal. 2012;58(8):2536-44.
20. Masoodi R, Pillai KM, Grahl N, Tan H. Numerical simulation of LCM mold-filling during the manufacture of natural fiber composites. Journal of Reinforced Plastics and Composites. 2012;31(6):363-78.
21. Francucci G, Rodríguez ES, Morán J. Novel approach for mold filling simulation of the processing of natural fiber reinforced composites by resin transfer molding. Journal of Composite Materials. 2014;48(2):191-200.
22. Mirnyy V, Clausnitzer V, Diersch H, Rosati R, Schmidt M, Beruda H. Wicking in absorbent swelling porous materials. Traditional and Modern Modeling Approaches, Wicking in Porous Materials. 2012:161-200.
23. Fluent A. Ansys fluent theory guide. ANSYS Inc, USA. 2011;15317:724-46.
24. Masoodi R, Pillai KM. Darcy's law-based model for wicking in paper-like swelling porous media. AIChE Journal. 2010;56(9):2257-67.
25. Javadi A, Pillai K, Sabo R. AN EXPERIMENTAL ESTIMATION OF LIQUID ABSORPTION COEFFICIENT FOR CELLULOSE NANO-FIBER FILMS2012.
26. Chattopadhyay K, Guthrie RI. Single Phase, Two Phase, and Multiphase Flows, and Methods to Model these Flows. Treatise on Process Metallurgy: Elsevier; 2014. p. 527-53.
27. Srinivasan V, Salazar AJ, Saito K. Modeling the disintegration of modulated liquid jets using volume-of-fluid (VOF) methodology. Applied mathematical modelling. 2011;35(8):3710-30.

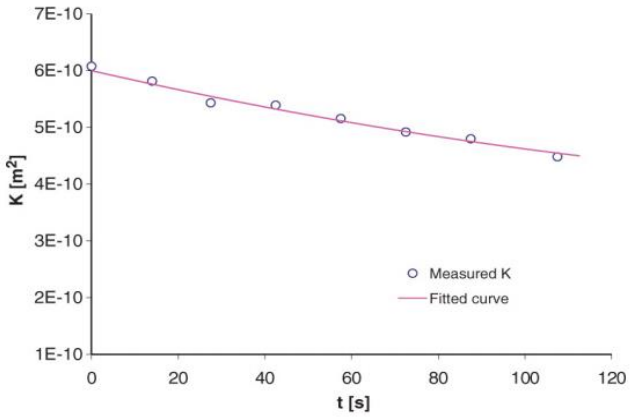

Figure 1 The measured changes in permeability of jute preform after getting wet[20]

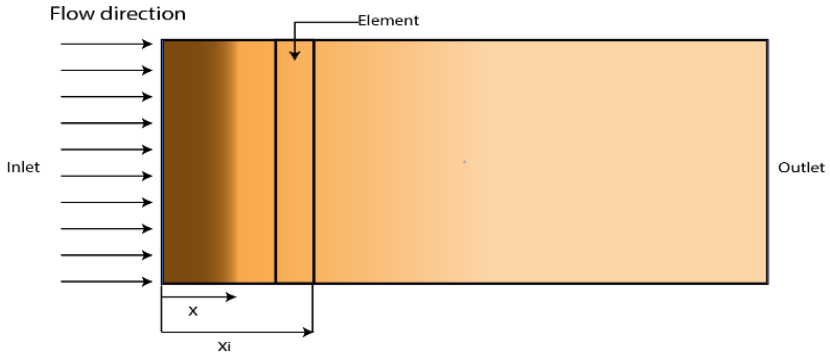

Figure 2 Problem setup for rectilinear flow in swelling porous medium

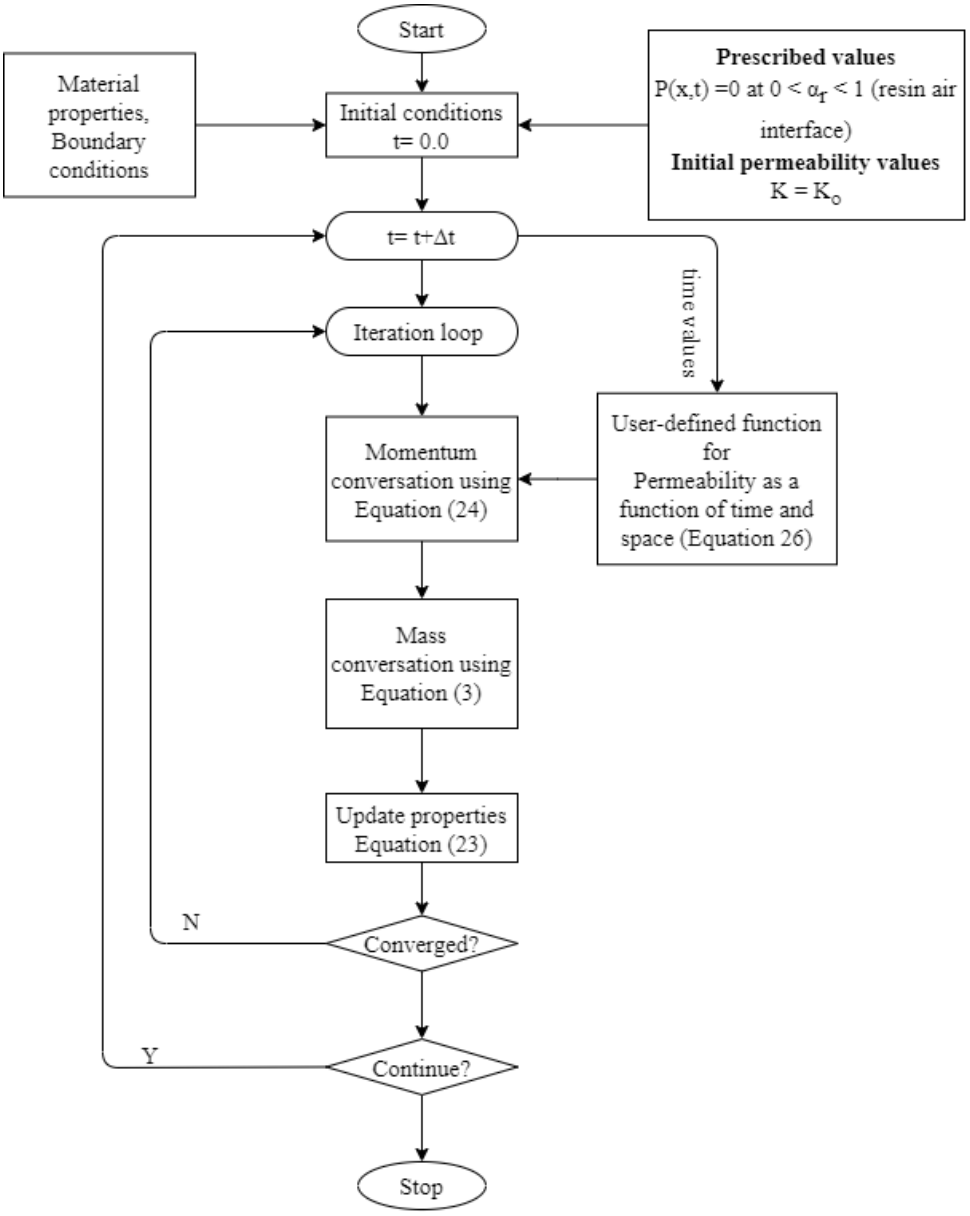

Figure 3 Numerical algorithm employing user-defined fuctions for present method

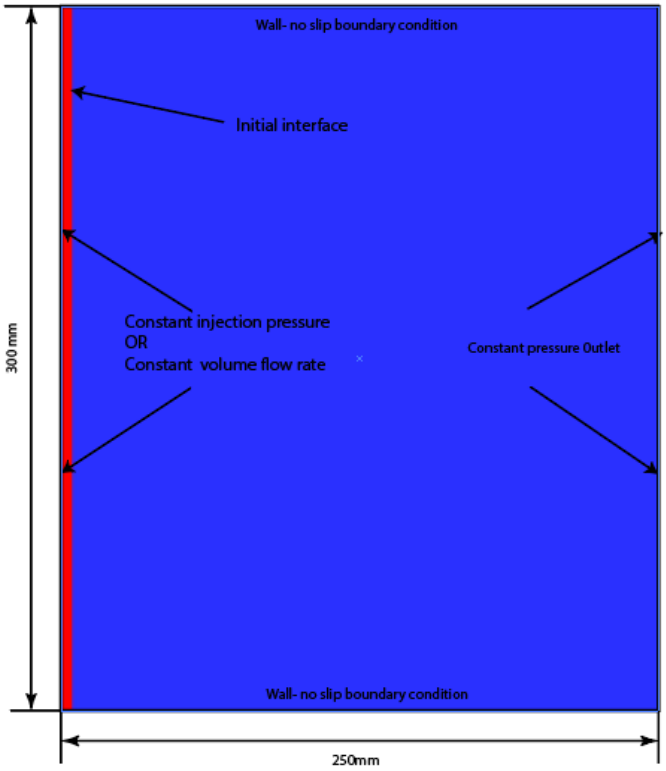

Figure 4 Details of Computational domain

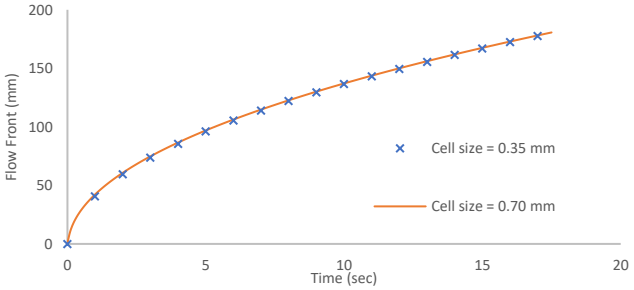

Figure 5 A comparison between Resin flow front locations for two different grid sizes (Constant inlet pressure case with 14 kPa as inlet pressure)

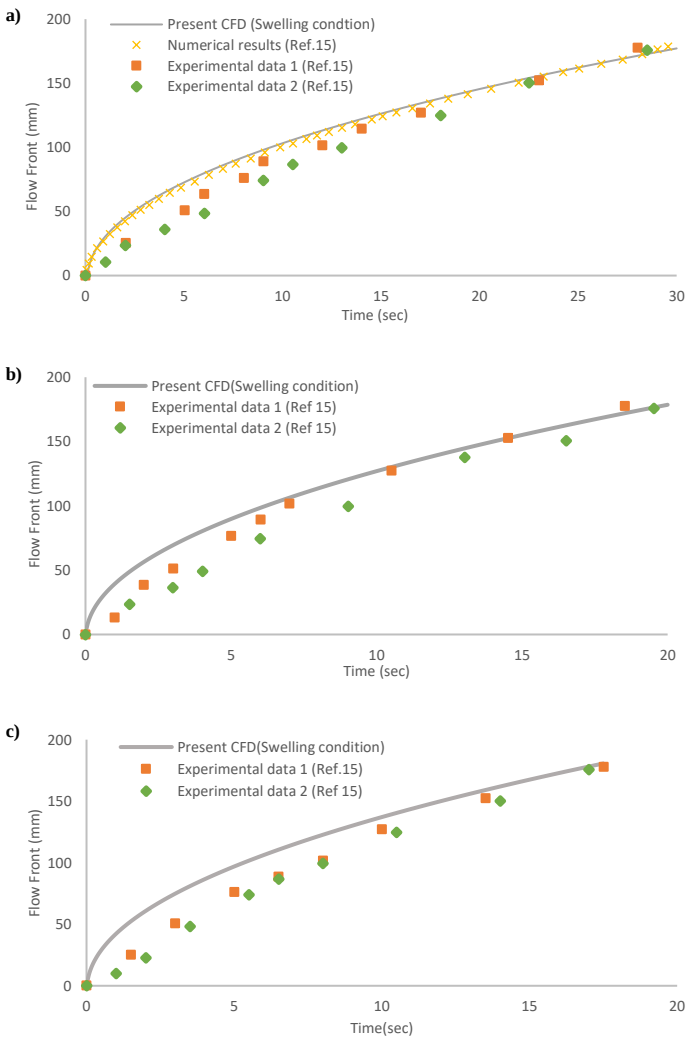

Figure 6 The comparision between experimental and CFD predictions for liquid-front locations for 1-D constant injection pressure conditions (a) p=8kPa (b) p=12kPa (c) p= 14kPa

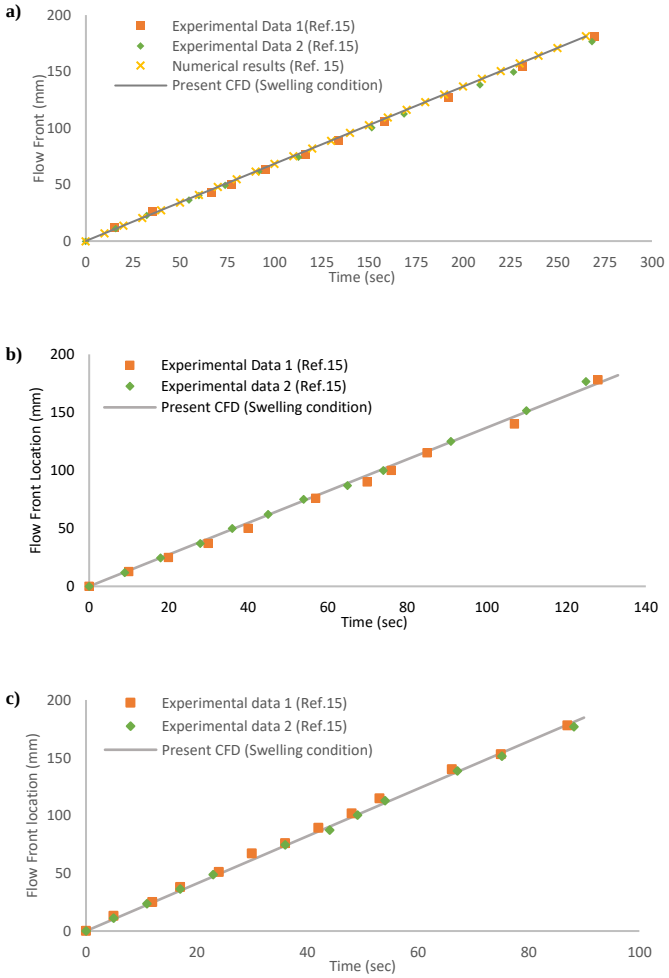

Figure 7 The CFD predictions for resin front locations for the 1-D constant volume flow rate condtions (a) Q = 1ml/s (b) Q = 2ml/s (c) Q = 3ml/s

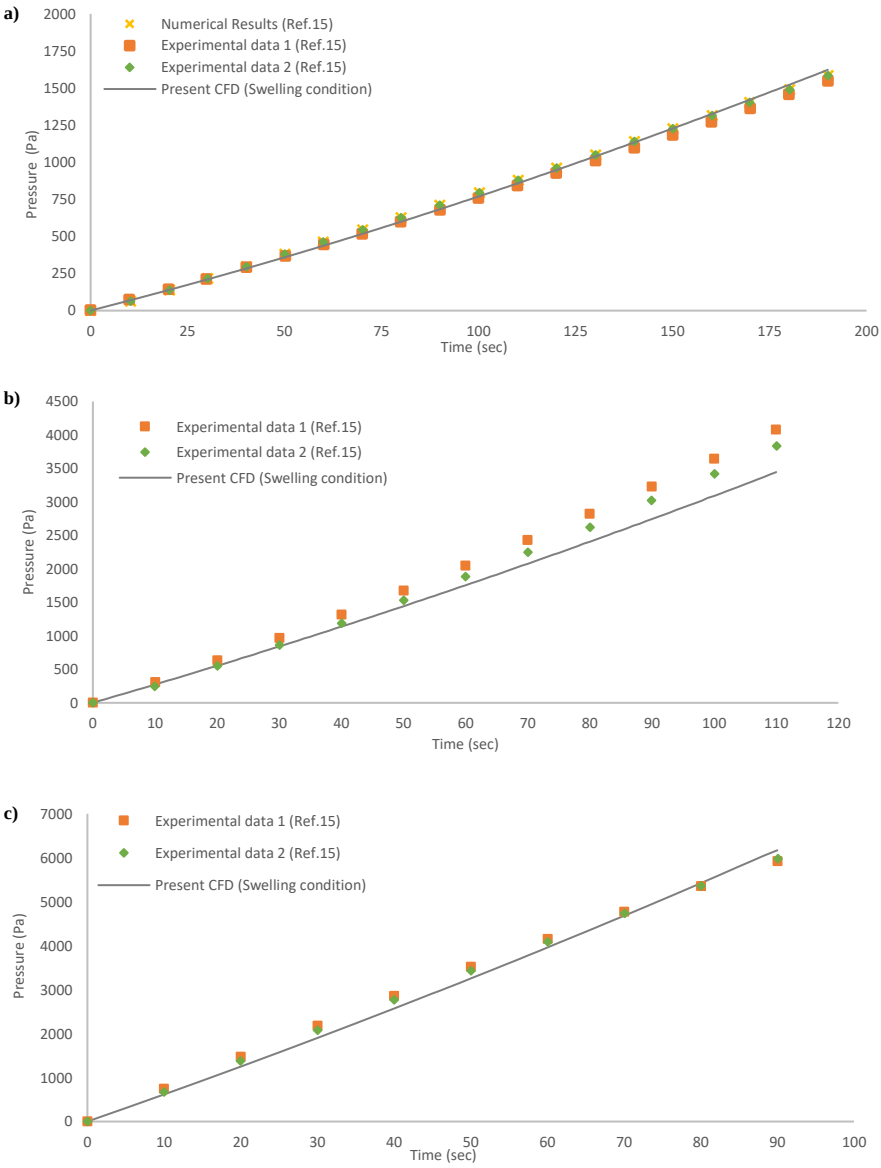

Figure 8 The Experimental and CFD predictions for the changes in the inlet pressure for constant volume flow rate conditions (a) Q = 1ml/s. (b) Q = 2 ml/s. (c) Q = 3 ml/s.

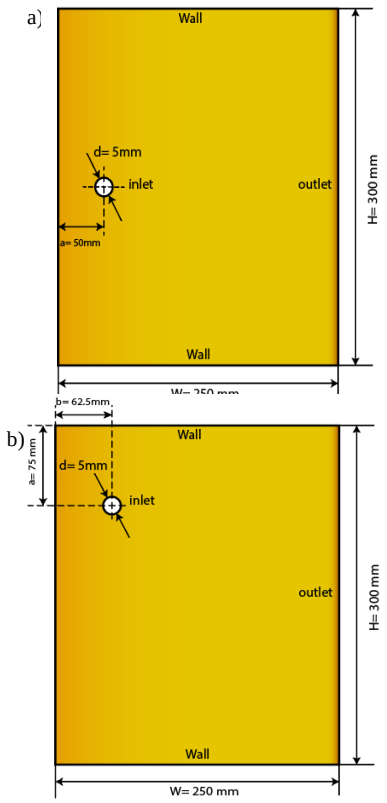

Figure 9 Geometrical details of the arrangements used for 2-D CFD simulation (a) Central injection arrangement (b) Eccentric injection arrangement

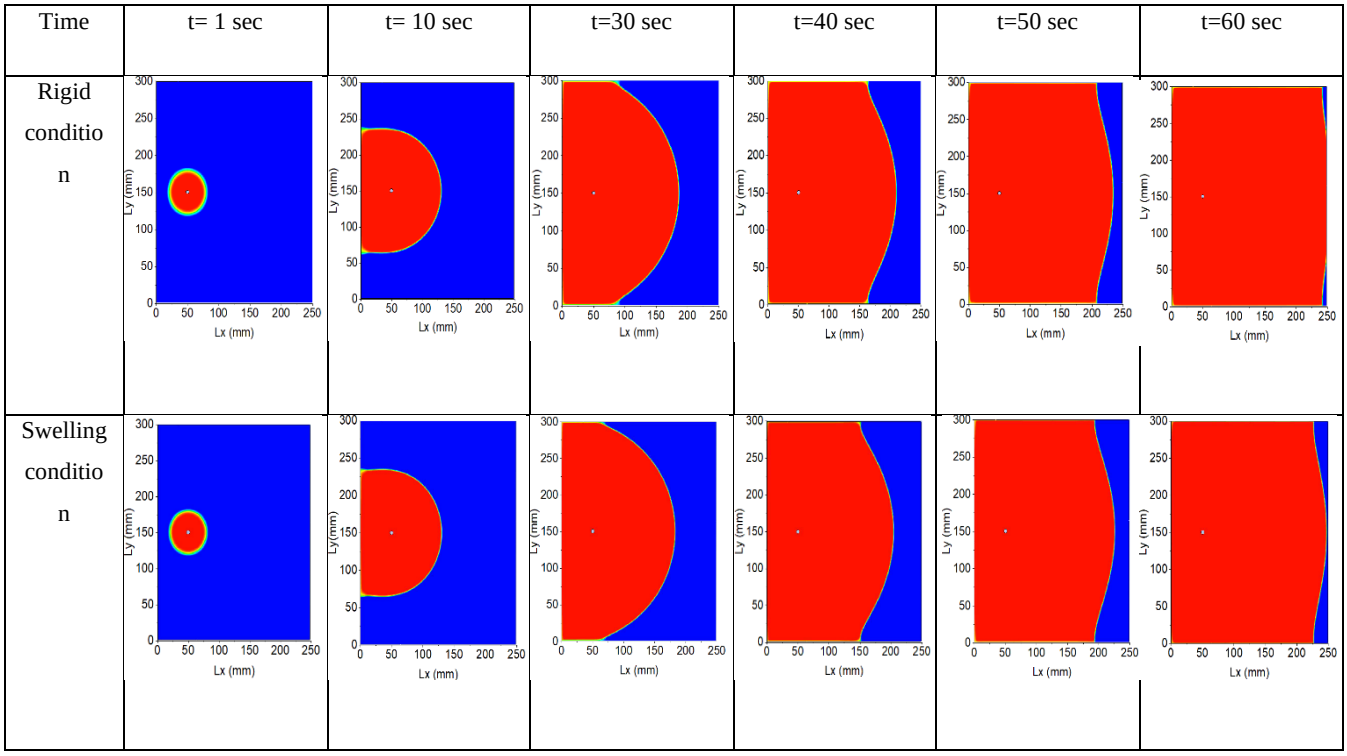

Figure 10 Transient contours of resin volume fraction for both rigid and swelling condition for 14 kPa inlet pressure case (Central injection case) (isotropic porous media)

Time	t= 1 sec	t= 10 sec	t=30 sec	t=50 sec	t=70 sec	t=100 sec
Rigid condition	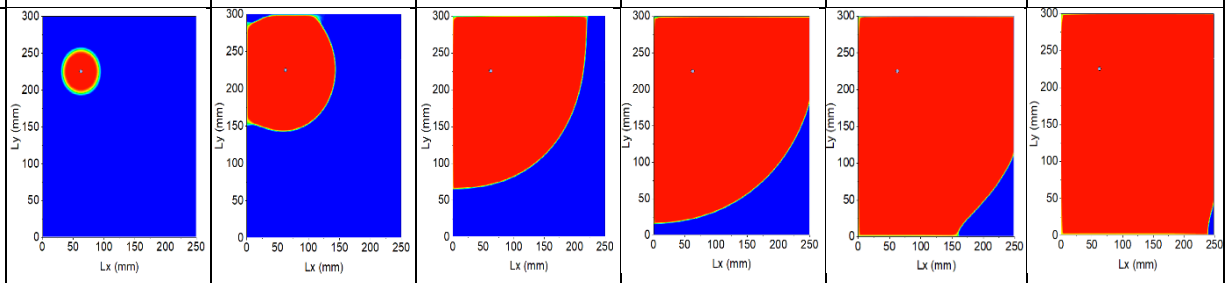					
Swelling condition	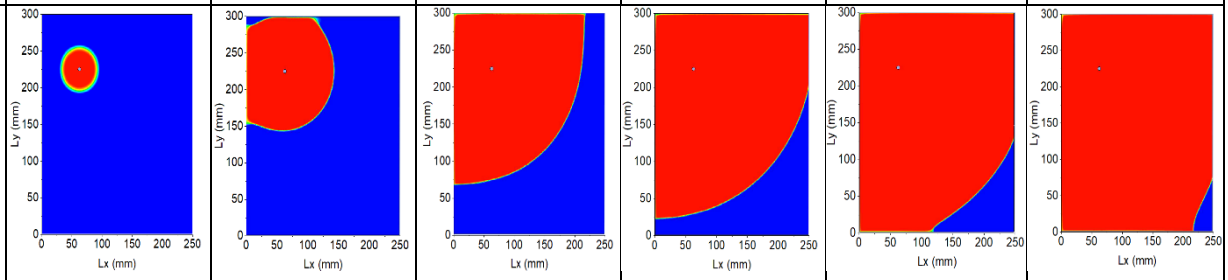					

Figure 11 Transient contours of resin volume fraction for both rigid and swelling condition for 14 kPa inlet pressure case (Eccentric injection case) (isotropic porous media)

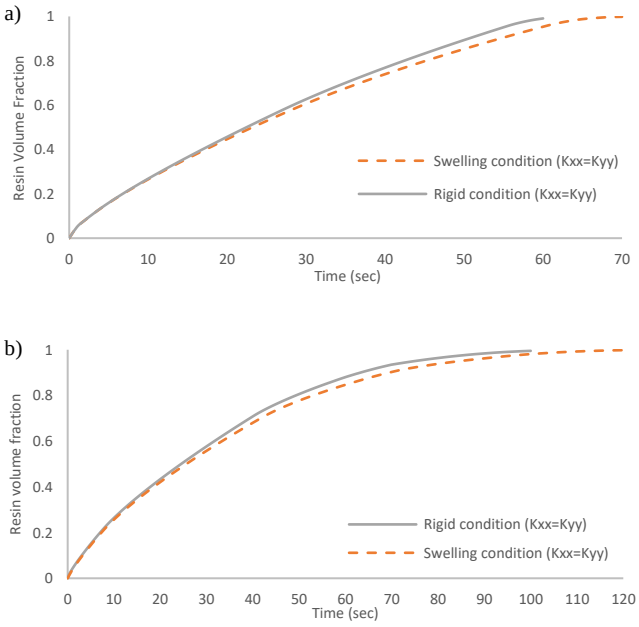

Figure 12 Plots of rein volume fraction Vs time for isotropic porous media (a) Central injection case (b) Eccentric injection case

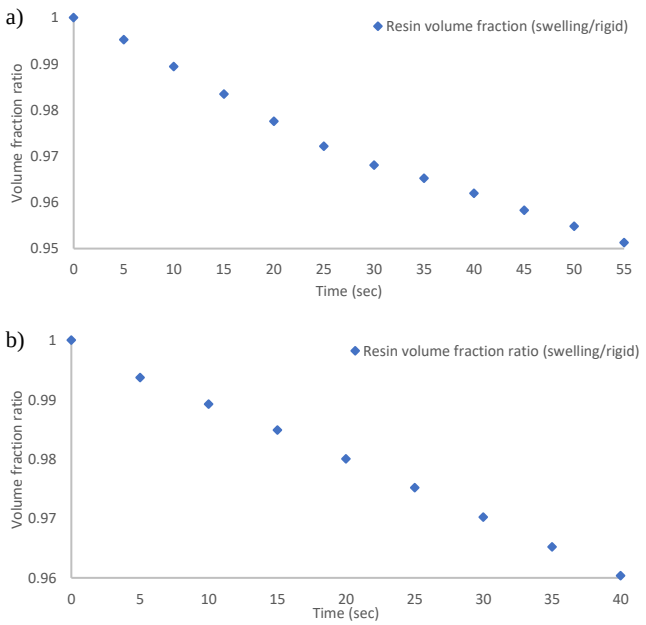

Figure 13 Plots of resin volume fraction ratio (Swelling/rigid) Vs time for isotropic porous media (a) Central injection case (b) Eccentric injection case

Time	t= 1 sec	t= 10 sec	t=50 sec	t=70 sec	t=90 sec	t=120sec
Rigid condition	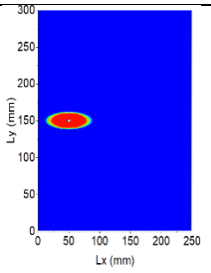	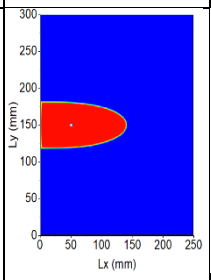	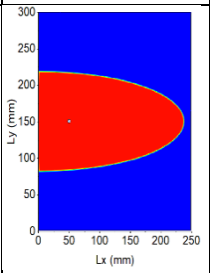	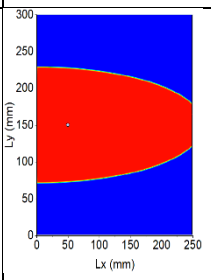	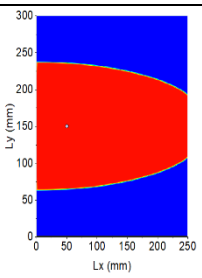	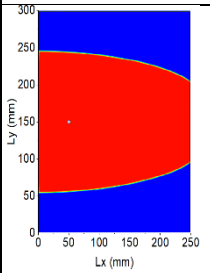
Swelling condition	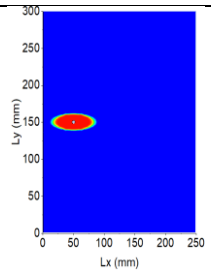	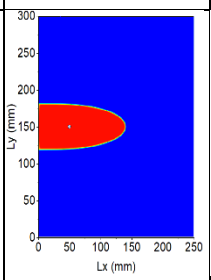	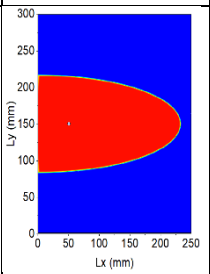	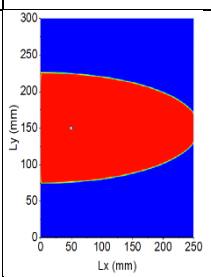	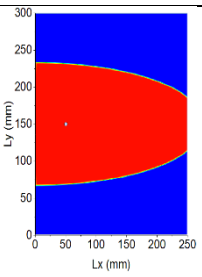	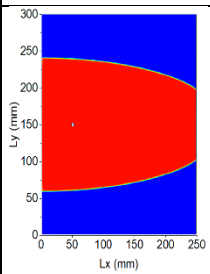

Figure 14 Transient contours of resin volume fraction for both rigid and swelling condition for 14 kPa inlet pressure case (Central injection case) (Orthotropic porous media)

Time	t= 1 sec	t= 10 sec	t=50 sec	t=70 sec	t=90 sec	t=120 sec
Rigid condition	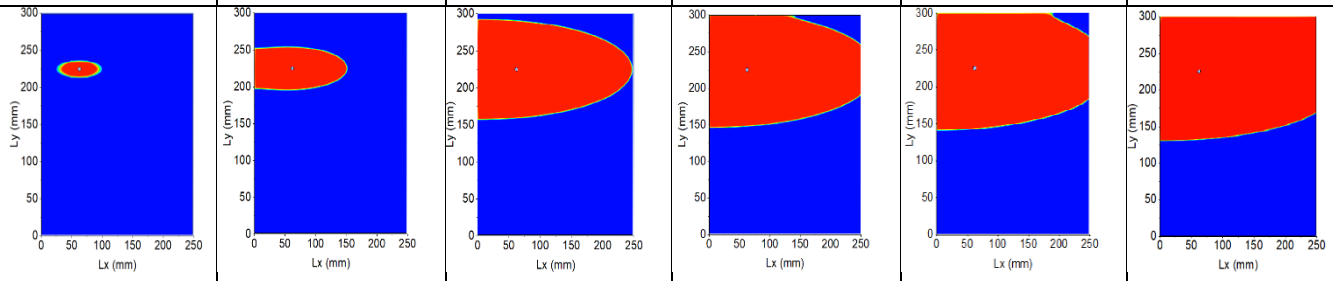					
Swelling condition	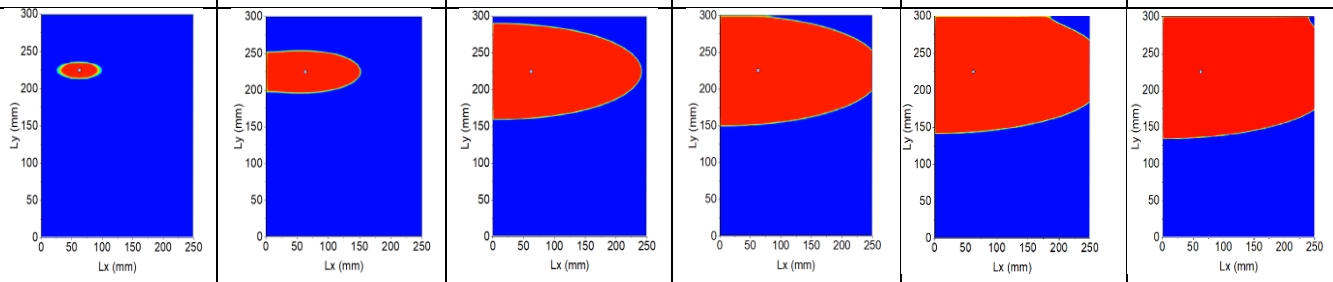					

Figure 15 Transient contours of resin volume fraction for both rigid and swelling condition for 14 kPa inlet pressure case (Eccentric injection case) (Orthotropic porous media)

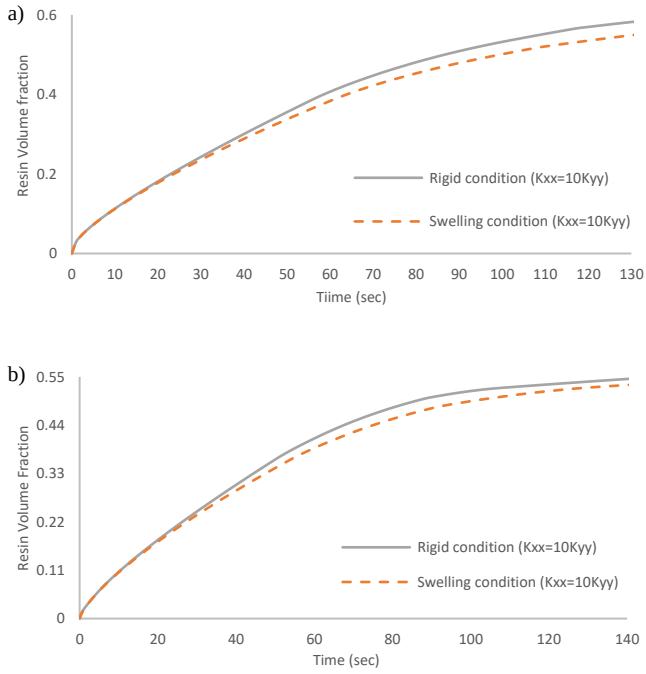

Figure 16 Plots of Rein volume fraction Vs time for Orthotropic porous media (a) Central injection case (b) Eccentric injection case

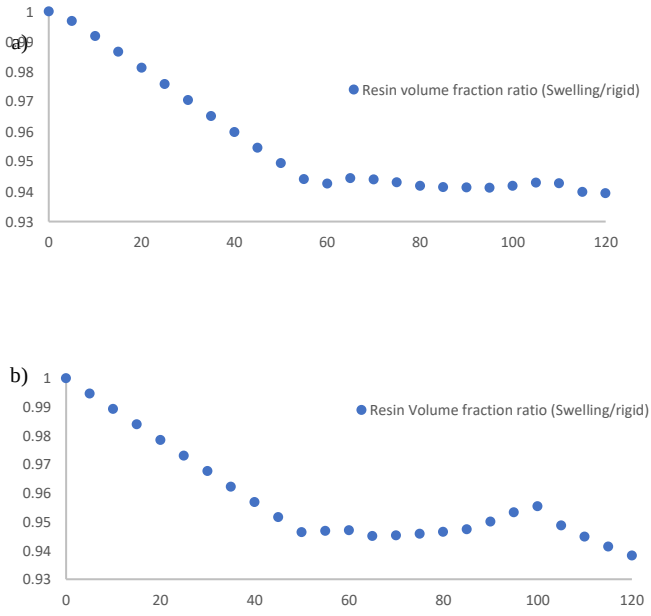

Figure 17 Plots of resin volume fraction ratio (Swelling/rigid) Vs time for Orthotropic porous media (a) Central injection case (b) Eccentric injection case

Table 1 Input parameters and modelling setup for CFD simulation

CFD setup condition		
General	Solver: Pressure-based transient	
Fluid materials	Air	**Viscosity**: 0.0179 Kg/m. s **Density:** 1.22Kg/m^3
	Resin (Test liquid)	**Viscosity:** 0.01 Kg/m. s **Density:** 1250 Kg/m^3
Cell zone condition	Permeability	**1. For isotropic conditions** **Rigid conditions:** $Kxx=Kyy=6\times10^{-10}$ m^2 **Swelling conditions:** $K_{xx}=K_{yy}$ =User-defined function based on equation (26) **2. For orthotropic conditions** **Rigid conditions:** $K_{xx}=6\times10^{-10}$ m^2 $K_{yy}=K_{xx}/10$ **Swelling conditions:** K_{xx} =User-defined function based on equation (26) $K_{yy}=K_{xx}/10$
	Porosity	**0.87**
Boundary conditions	Inlet (For constant inlet pressure) Inlet (For constant flow rate) Outlet at Flow Front [6]	**8kPa,12kPa and 14kPa** **1ml/sec, 2ml/sec and 3ml/sec.** **Atmospheric pressure. P=0**
Model	Viscous flow model: Laminar Multiphase model: Volume of Fluid	**Phase 1:** Air **Phase 2:** Resin